Structural Engineering and Mechanics, Vol. 39, No. 6 (2011) 813-831
DOI: http://dx.doi.org/10.12989/sem.2011.39.6.813

A hybrid algorithm based on EEMD and EMD for multi-mode signal processing

Jeng-Wen Lin*

Department of Civil Engineering, Feng Chia University, Taichung, Taiwan 407, R.O.C.

(Received January 26, 2011, Accepted June 22, 2011)

Abstract. This paper presents an efficient version of Hilbert-Huang transform for nonlinear non-stationary systems analyses. An ensemble empirical mode decomposition (EEMD) is introduced to alleviate the problem of mode mixing between intrinsic mode functions (IMFs) decomposed by EMD. Yet the problem has not been fully resolved when a signal of a similar scale resides in different IMF components. Instead of using a trial and error method to select the "best" outcome generated by EEMD, a hybrid algorithm based on EEMD and EMD is proposed for multi-mode signal processing. The developed approach comprises the steps from a bandpass filter design for regrouping modes of the IMFs obtained from EEMD, to the mode extraction using EMD, and to the assessment of each mode in the marginal spectrum. A simulated two-mode signal is tested to demonstrate the efficiency and robustness of the approach, showing average relative errors all equal to 1.46% for various noise levels added to the signal. The developed approach is also applied to a real bridge structure, showing more reliable results than the pure EMD. Discussions on the mode determination are offered to explain the connection between mode-grouping form on the one hand, and mode-grouping performance on the other.

Keywords: ensemble empirical mode decomposition; filter design; intrinsic mode function; multi modes; signal processing

1. Introduction

Hilbert-Huang transform (HHT), i.e., empirical mode decomposition (EMD) and the Hilbert transform (Huang *et al*. 1998, Huang *et al*. 2003), has received a wide variety of attention and application in many fields. Applying EMD to the signal will produce intrinsic mode functions (IMFs), each represents a physical meaning for the system. Then applying the Hilbert transform to convert the IMFs into the frequency domain in a time-frequency-amplitude display makes the HHT sophisticated and versatile.

However, one of the major drawbacks of the EMD is the frequent appearance of mode mixing, which is defined as a single IMF either consisting of signals of widely disparate scales, or a signal of a similar scale residing in different IMF components (Wu and Huang 2009). When the problem of mode mixing occurs, an IMF can cease to have a physical meaning by itself, suggesting falsely that there may be different physical processes represented in a mode (Wu and Huang 2009, Lei and Zuo 2009). This mode mixing was initially avoided by an "intermittency" test (Huang *et al*. 1999),

*Corresponding author, Associate Professor, E-mail: jwlin@fcu.edu.tw

in which a criterion based on the period length was introduced to separate the waves of different periods into different modes. The criterion was set as the upper limit of the period that can be included in any given IMF component, so that the intermittent small wave was separated from the large waves. Xu *et al*. (2003) also used the intermittence check to avoid mode mixing for the modal identification of Di Wang Building. This intermittence check could be accomplished by specifying a cutoff frequency for each IMF during its sifting process, where data with frequencies lower than the cutoff frequency would be removed from the resulting IMF, but such a check should be applied with care due to its subjective condition added to the EMD sifting process. Later, Wu and Huang (2009) proposed an ensemble EMD (EEMD) method to alleviate the mode mixing problem. The EEMD defines the true IMF components as the mean of an ensemble of trials, each consisting of the signal plus a white noise of finite amplitude. Although the new technology EEMD was developed in recent years, it has been applied in various fields.

For example, Li *et al*. (2008) used the EEMD based hybrid power load forecasting method to solve the mode mixing problem frequently appearing in classical empirical mode decomposition and to rectify the common-used load analyzing methods mostly relying on subjective experiences. Zhang *et al*. (2008) extended the EEMD to crude oil price analysis. Yeh *et al*. (2008) proposed a complementary ensemble empirical mode decomposition method (CEEMD) to solve the problems of end effects and the phenomenon of intermittence. Chen *et al*. (2009) proposed that the pipeline flaw magnetic flux leakage signal was extracted using the EEMD and the sparsity. Wu and Chung (2009) investigated the feasibility of utilizing the hybrid method of EEMD and pure EMD to efficiently decompose the complicated vibration signals of rotating machinery into a finite number of IMFs, so that the fault characteristics of the misaligned shaft can be examined in the time-frequency Hilbert spectrum as well as the marginal Hilbert spectrum. Zhou *et al*. (2009) utilized the EEMD to adaptively reduce noise and remove background intensity from a two-dimensional fringe pattern.

Although the EEMD can alleviate the mode mixing problem, the problem has not been fully resolved especially when a signal of a similar scale (frequency) resides in different IMF components. Wu and Huang (2009) pointed out that the problem associated with the EEMD was how to treat multi-mode distribution of the IMFs. As discussed by Gledhill (2003), the discrepancy between a trial and its reference tended to show a bi-modal (if not multi-modal) distribution. The true cause of the problem could be explained based on the studies of white noise using the EMD (Flandrin *et al.* 2004, Wu and Huang 2004), in which the EMD was effectively a dyadic filter bank showing some overlap in scales. Signals having a scale located in the overlapping region would have finite probability appearing in two different modes. Lei and Zuo (2009) suggested selecting the one generating the “best” result of EEMD after having tried noise levels (its standard deviation values) in the range from 0 to 30% with a step size of 1%. However, such a “trial and error” method requires a considerable amount of time to train the EEMD algorithm. On the other hand, Wu and Huang (2009) suggested three alternative implementations of the sifting procedures to alleviate its severity. The first alternative was to tune the noise level and used more trials to reduce the RMS deviation. The second alternative was to sift a low but fixed number of times (e.g., 10 times) for obtaining each IMF components. The third alternative was to use rigorous check of the each component against the definition, and divided the outcome into different groups according to the total number of IMF generated. Furthermore, the first and second alternatives had been tried and the consequences showed that none could avoid the multi-mode problem totally. The true solution might have to combine the multi-mode into a single mode, and sifted it again to produce a proper single IMF (Wu and Huang 2009).

Based on these arguments, this study aims to (1) assess the performance of EEMD by an orthogonality check on each resulting IMF, and (2) compare the grouping efficiency of IMFs generated by EEMD with that of the bandpass-EMD based approach (Lin 2010) for the multi-mode signal processing. First, a historical account of the development of EEMD is provided. Second, the bandpass-EMD approach is applied to the combined IMFs generated by EEMD, so as to produce proper IMFs for the mode determination. The proposed approach comprises the steps from a bandpass filter design for regrouping modes of the new signal obtained from EEMD, to the mode extraction using EMD, and to the accurate assessment of a single mode in the frequency spectrum. Third, a simulated signal with two-modes is tested to demonstrate the efficiency of the proposed approach. A linear sum of two cosine waves to form a two-mode signal possessing similar scales is considered. To embark the EEMD process, various noise levels with a standard deviation of 0%, 5%, 10%, 20%, and 40% are added to the signal, respectively. The signal is then decomposed into a variety of IMFs using EEMD, followed by combining the multi-mode into a single mode, and sifting it again to produce proper IMFs one by one using the bandpass-EMD based approach, which divides the outcome into different groups. The resulting evaluated frequencies of the two-mode signal are compared with the real values. Application of the proposed approach to a real bridge structure is also conducted. Finally, discussions on the determination of modes are offered to explain the connection between mode-grouping form and type on the one hand, and mode-grouping performance on the other.

2. Methodology: a hybrid algorithm based on EEMD and EMD

Fig. 1 illustrates the hybrid algorithm based on EEMD and EMD (with the assistance of the EMD/EEMD evaluation code by Wu and of the Hilbert spectrum evaluation code by Gabriel.Rilling (at) ens-lyon.fr), which consists of (1) the EEMD to alleviate the mode mixing problem, (2) the design of a bandpass filter to fully resolve the mode mixing problem, (3) the mode extraction using EMD, and (4) the modal frequency estimation in the marginal spectrum. First, a historical account of EEMD is provided. The EEMD is an improved version of EMD using an ensemble average of IMFs decomposed by EMD. The EMD associated with the Hilbert transform comprises the Hilbert-Huang transform (HHT) (Huang *et al.* 1998, Huang *et al.* 2003).

2.1 Hilbert-Huang transform

The Hilbert transform for an arbitrary time series $x(t)$ can be defined by $y(t)$ as

$$y(t) = \frac{1}{\pi}\int_{-\infty}^{\infty} \frac{x(t)}{t-\tau} d\tau \tag{1}$$

which is the convolution of the signal $x(t)$ with $1/t$, and the associated analytic signal $z(t)$ of $x(t)$ is described by

$$\begin{cases} z(t) = x(t) + iy(t) = a(t)e^{i\theta(t)} \\ a(t) = \sqrt{x^2(t) + y^2(t)} \\ \theta(t) = \arctan(y(t)/x(t)) \end{cases} \tag{2}$$

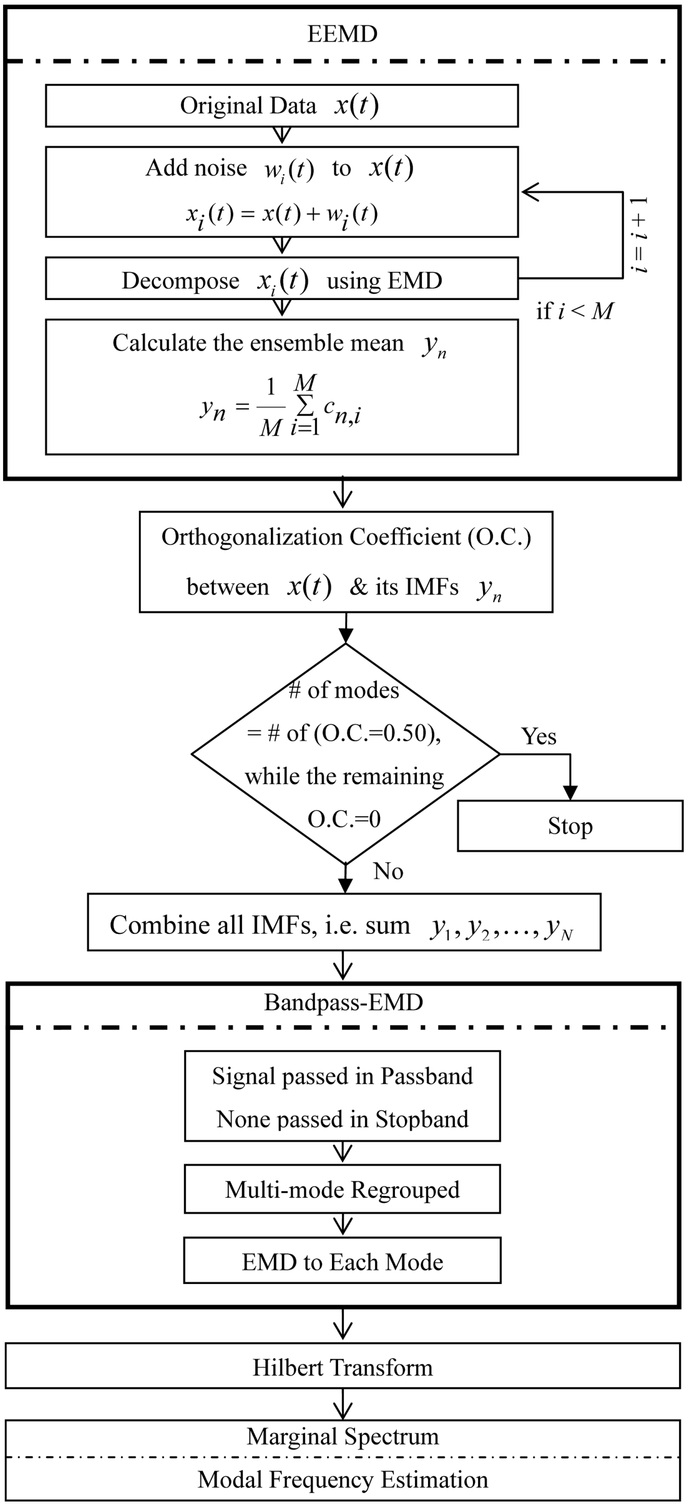

Fig. 1 The hybrid algorithm based on EEMD and EMD for multi-mode signal processing

By using these expressions, the time-frequency-amplitude relationship of the signal can be adequately represented. Since the phase $\theta(t)$ is a function of time t, the frequency will be a function of time by taking the derivative of $\theta(t)$ to yield the instantaneous frequency (Huang *et al.* 1998) as

$$\omega(t) = \frac{d\theta(t)}{dt} \tag{3}$$

The EMD method can decompose a signal into a collection of individual and almost monocomponent signals called intrinsic mode functions (IMFs) (Huang *et al.* 1998). The EMD process can be summarized as follows (Huang *et al.* 1999, Peng *et al.* 2005)

(a) Initialize $r_0 = x(t)$, and $n = 1$;
(b) Extract the nth IMF (i.e., c_n, $n = 1, 2, \ldots, N$) by
  (1) Initialize $h_{n(k-1)} = r_{(n-1)}$, $k = 1$;
  (2) Connect all the local maxima of $h_{n(k-1)}$ by a cubic spline line as the upper envelope of $h_{n(k-1)}$, and repeat the procedure for the local minima to produce the lower envelope;
  (3) Calculate the local mean m_{nk} of the upper and lower envelopes of $h_{n(k-1)}$;
  (4) Repeat the sifting up to k times, and designate $h_{nk} = h_{n(k-1)} - m_{nk}$;
  (5) If h_{nk} is an IMF, set $c_n = h_{nk}$; otherwise go to step (2) with $k = k+1$;
(c) Define $r_n = r_{n-1} - c_n$ $(n = 1, 2, \ldots, N)$;
(d) If r_n becomes a monotonic function, the EMD process is stopped; otherwise go to step (b) with $n = n+1$.

The EMD method is adopted to resolve the signal $x(t)$ into the final form as

$$x(t) = \sum_{n=1}^{N} c_n(t) + r_N(t) \tag{4}$$

where $c_n(t)$ $(n = 1, 2, \ldots, N)$ are the IMFs and $r_N(t)$ is the residue of $x(t)$. The IMF is a mode function characterizing: (1) in the whole data set, the number of extrema and the number of zero-crossings must either equal or differ at most by one; and (2) at any point, the mean value of the envelope defined by local maxima and the envelope defined by the local minima is zero (Huang *et al.* 1999). An IMF represents a simple oscillatory mode embedded in the signal. With the simple assumption that any signal consists of different simple IMFs, the EMD method is able to decompose a signal into IMFs (Lei and Zuo 2009).

After employing the Hilbert transform on each IMF by using Eqs. (1)-(4), it is possible to express the signal $x(t)$ (Huang *et al.* 1998) as

$$x(t) = \sum_{n=1}^{N} a_n(t) \exp\left(i \int \omega_n(t) dt\right) \tag{5}$$

Using Eq. (5), one can represent the variable amplitude $a_n(t)$ on the time-frequency plane to yield the Hilbert spectrum $H(\omega, t)$. Hence, the Hilbert transform with EMD is able to generate the time-frequency-amplitude distribution to describe the signal $x(t)$. The Hilbert spectrum can be integrated with respect to time to give the marginal spectrum as

$$h(\omega) = \int_0^T H(\omega, t) dt \tag{6}$$

The marginal spectrum provides a measure of total amplitude (or energy) contribution from each frequency value (Huang *et al*. 1998).

2.2 Ensemble empirical mode decomposition

Because the IMFs of a signal derived from the EMD will often engender the mode mixing problem for a relatively wide band signal, Wu and Huang (2009) proposed an EEMD to alleviate this problem. The upper portion of Fig. 1 illustrates the flow chart of EEMD, described as follows (Wu and Huang 2009, Lei and Zuo 2009):

(a) Add a white noise series to the targeted data. The added white noise is treated as the possible random noise that would be encountered in the measurement process. Under such conditions, the i-th "artificial" observation will be

$$x_i(t) = x(t) + w_i(t) \tag{7}$$

in which $x_i(t)$ is the observational data, $x(t)$ is the true signal, and $w_i(t)$ is the noise. Thus, all data are amalgamations of signal and noise. Although adding noise may result in smaller signal-to-noise ratio, the added white noise will provide a relatively uniform reference scale distribution to facilitate EMD; therefore, the low signal-noise ratio does not affect the decomposition method but actually enhances it to avoid the mode mixing (Wu and Huang 2009).

(b) Utilize the EMD to decompose the signal with added white noise into N IMFs, $c_{n,i}$ $(n = 1, 2, \ldots, N)$, where $c_{n,i}$ denotes the nth IMF of the ith trial, and N is the number of IMFs.

(c) Repeat step (a) and step (b) again and again, but with different white noise series each time.

(d) Obtain the (ensemble) means of corresponding IMFs of the decompositions as the final result. The ensemble means y_n of the M trials for each IMF is defined as

$$y_n = \frac{1}{M}\sum_{i=1}^{M} c_{n,i}, \quad n = 1, 2, \ldots, N \quad i = 1, 2, \ldots, M \tag{8}$$

where the mean y_n $(n = 1, 2, \ldots, N)$ of each of the N IMFs is calculated as the final IMF.

If the added noise amplitude is relatively small, it may not introduce the change of extrema that the EMD relies on. By increasing the ensemble members, the effect of the added white noise can be reduced to a negligibly small level. In general, an ensemble number of a few hundred will lead to a very good result, and the remaining noise would cause less than a fraction of 1% of error if the added noise has the amplitude that is a fraction of the standard deviation of the original data (Wu and Huang 2009). In real-life applications, however, an appropriate noise level should be selected to produce the best result of EEMD. For instance, Lei and Zuo (2009) tried various noise levels ranging from 0 to 30% with a step size of 1%, and the noise level producing the best result was selected.

2.3 Design of a bandpass-EMD filter

Although EEMD could alleviate the mode mixing problem, the EEMD appears to be less effective when a signal contains two or more similar scales (frequencies). If the "best" result of various trials generated by EEMD is not satisfactory, the following step can be adopted. The criterion developed to check whether the EEMD outcomes are satisfactory or not relies on that the number of modes of $x(t)$ is equal to the number of the orthogonalization coefficient (Huang *et al.* 1998) between the signal $x(t)$ and its IMFs y_n generated by EEMD being equal to 0.50 (round-off value) while the remaining orthogonalization coefficients being equal to zero, as shown in Fig. 1. The orthogonalization coefficient ranges from 0 to 0.5 and is defined as

$$\mathrm{IO}_{fg} = \sum_{t} \frac{C_f C_g}{C_f^2 + C_g^2} \tag{9}$$

where IO_{fg} denotes the index of orthogonality between the two signals, C_f and C_g.

If the criterion is satisfied, the overall signal processing procedure can be stopped. Otherwise, the bandpass-EMD filtering approach (Lin 2010) should be followed and applied to the signal containing combined IMFs generated by EEMD. The filtering approach comprises the steps from a bandpass filter design for separating and regrouping modes of the IMFs obtained from EEMD, to the mode extraction using EMD, and to the accurate assessment of a single mode in the frequency spectrum. The bandpass filter is utilized to regroup and extract the modes of the signal containing combined IMFs (i.e., $\sum_{n=1}^{N} y_n$). The bandpass filter uses a cutoff frequency that corresponds in amplitude to 10% of the peak value for the signal in the frequency spectrum (Etter 1993). There is no transition band between the passband and the stopband for the designed filter, i.e., the cutoff frequency equals the rejection frequency. The signal is only allowed oscillations between the cutoff frequencies, and amplitudes in other intervals are set to zero so as to filter out lower and higher portions of the signal arising from measurement errors (Lin 2010).

After the signal is undergone the bandpass filter, the wide band signal to be processed is regrouped into a series of narrow band signals, each representing one mode. Each mode is further processed using the orthogonalization coefficient, Eq. (9), to select a most appropriate IMF among the IMFs obtained from the EMD of the signal's mode. The IMF possessing the highest orthogonalization coefficient between the signal's mode and its IMFs (usually equal to 0.50 round-off value) is selected to represent the modal signal. Each IMF that represents a modal signal can be obtained sequentially according to the number of modes of $x(t)$.

3. Numerical examples and analyses

3.1 Evaluation of a two-mode signal

A simulated signal with two-modes is tested to demonstrate the efficiency of the proposed approach. A linear sum of two cosine waves (Huang *et al.* 1998) to form a two-mode signal containing similar scales is considered and described in Eq. (10) over t from 1-512 s, with the time interval Δt = 0.1 s. The real frequency values are 1/34 (0.02941) Hz and 1/30 (0.03333) Hz.

$$x(t) = \cos\frac{2}{30}\pi t + \cos\frac{2}{34}\pi t \tag{10}$$

In order to understand the impact of noise on the EEMD outcome, the noise level with a standard deviation of 0%, 5%, 10%, 20%, and 40% is added to the signal, respectively. It is noted that adding 0% noise level to the signal to undergo the EEMD process is equivalent to the signal to directly undergo the EMD process. The upper left portion of Fig. 2 shows the time history of the original signal. The signal is decomposed into IMFs using EEMD, followed by combining the

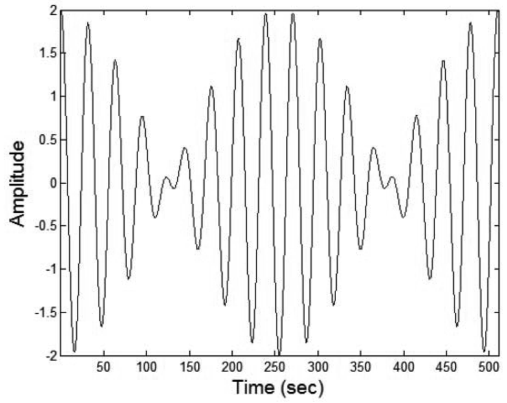

Original signal

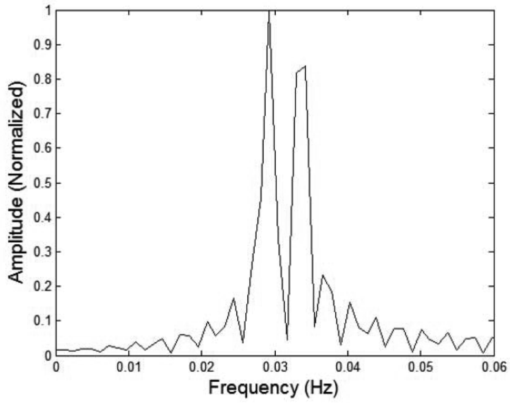

Fourier spectrum of original signal

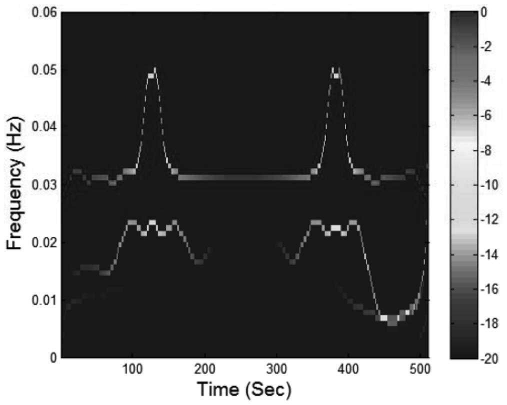

Hilbert spectrum of original signal

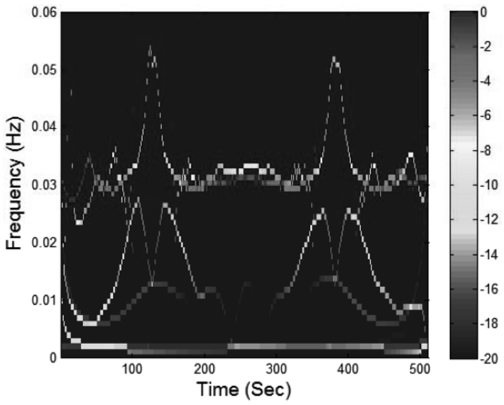

Hilbert spectrum after EEMD

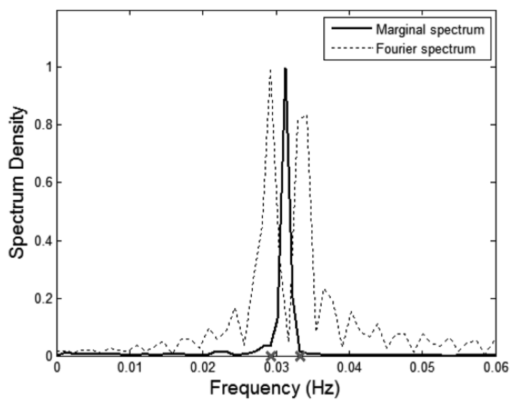

Marginal spectrum of original signal

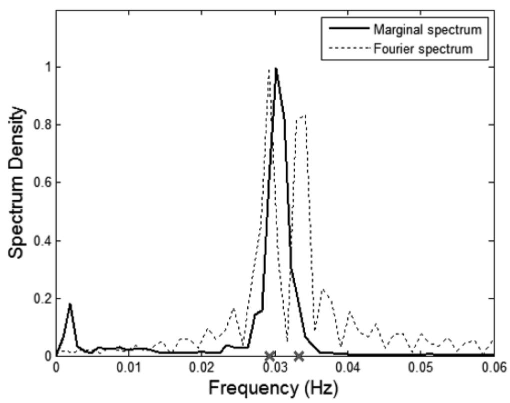

Marginal spectrum after EEMD

Fig. 2 The outcomes, including the Hilbert spectra and marginal spectra, of EEMD for the cases of 0% (left portion) and 20% (right portion) noise levels, respectively (× indicate the real modal frequencies)

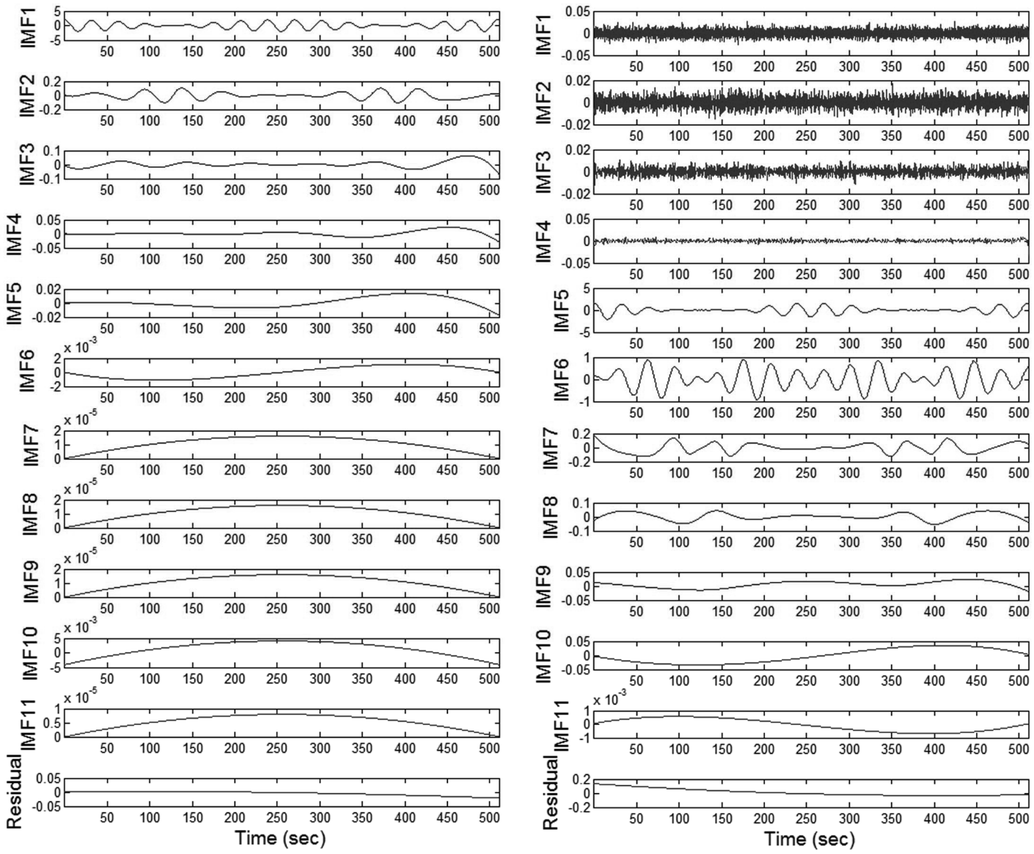

Fig. 3 The decomposed IMFs using EEMD: the left and right portions are for the signal with 0% and 20% noise levels, respectively

multi-mode into a single mode, and sifting it again to produce a proper single IMF as a mode using the bandpass-EMD based algorithm, which divides the outcome into different groups to find modes one by one. The estimated frequencies of the two-mode signal are compared with the real values.

First, the EEMD is applied to the two-mode signal to result in a variety of IMFs that are the ensemble means of 500 trials of EMD. Fig. 3 shows the decomposed IMFs using EEMD: the left and right portions are for the signal with 0% and 20% noise level, respectively. Table 1 lists the orthogonalization coefficients between the signal and the decomposed IMFs using EEMD with 0%, 5%, 10%, 20%, and 40% noise levels, respectively. The number of "distinguished" orthogonalization coefficients (in bold) in each noise level (except for the 0% noise level which refers to the EMD procedure) is two, implying that the possible mode number is two. This mode number determination is clarified and discussed in the next section.

Fig. 2 shows the outcomes, including the Hilbert spectra and marginal spectra, of EEMD for the cases of 0% and 20% noise levels, respectively. In particular, the upper right portion of Fig. 2 shows the Fourier spectrum of the original signal, suggesting that two modes exist in the original signal. Hilbert spectra also suggest that two modes exist in the signal, but the spectrum becomes noisier when the 20% noise level is added. However, the marginal spectra appear to have one

Table 1 Orthogonalization coefficients between the signal and the decomposed IMFs using EEMD with 0%, 5%, 10%, 20%, and 40% noise levels, respectively

	0% Noise	5% Noise	10% Noise	20% Noise	40% Noise
Self	0.5	0.5	0.5	0.5	0.5
IMF1	**0.4995**	0.0000	0.0000	0.0000	0.0000
IMF2	0.0046	0.0000	0.0000	0.0001	0.0001
IMF3	-0.0009	0.0000	0.0000	0.0000	0.0001
IMF4	-0.0004	**0.2589**	0.0136	0.0000	0.0000
IMF5	-0.0002	**0.4511**	**0.4919**	**0.4334**	**0.1179**
IMF6	0.0000	0.0077	**0.0605**	**0.3017**	**0.4859**
IMF7	0.0000	-0.0001	0.0045	0.0068	0.0200
IMF8	0.0000	-0.0004	-0.0004	-0.0010	0.0024
IMF9	0.0000	0.0000	0.0000	-0.0003	0.0004
IMF10	0.0000	0.0000	0.0000	0.0000	0.0002
IMF11	0.0000	0.0000	0.0000	0.0000	0.0000
Residual	-0.0002	-0.0003	-0.0004	-0.0001	0.0006

"averaged" peak of distribution, suggesting only one mode existing in the original signal. Although there are two peaks for the case of 20% noise level, suggesting two modes existing in the original signal, the smaller peak value is negligible and in fact only one mode can be identified. Hence, the mode mixing problem has not been fully resolved using EEMD when a signal contains similar scales or a signal of a similar scale (frequency) resides in different IMF components, as shown in Fig. 3.

Although it might happen to select the one with the noise level generating the "best" result of EEMD (Lei and Zuo 2009) through a rigorous check of the orthogonalization coefficient described in section 2.3, the chance is relatively small. The true solution might have to combine the multi-mode into a single mode, and sifted it again to produce a proper single IMF (Wu and Huang 2009). Thus, the IMFs generated by EEMD have been regrouped. Fig. 4 shows the Hilbert spectra and marginal spectra of the signal containing combined all IMFs generated by EEMD with 20% noise level (left portion) and the correspondingly filtered signal after the bandpass-EMD filter (right portion), respectively. Fig. 5 shows the decomposed IMFs of the signal containing combined all IMFs, which is different from the one in Fig. 3. However, the condition that a signal of a similar scale (frequency) resides in different IMF components has not yet improved. Such a mode mixing condition also reflects on the orthogonalization coefficients between the signal containing combined all IMFs generated by EEMD with 0%, 5%, 10%, 20%, and 40% noise levels, respectively, and the decomposed IMFs, as listed in Table 2.

The problem of mode mixing is not yet resolved until the bandpass-EMD filter is adopted. The bandwidth (0.0098 Hz for mode 1 and 0.0037 Hz for mode 2) of the bandpass filter is very small compared to the sampling frequency ($1/\Delta t$ = 10 Hz), indicating that the filter is a narrowband design for extracting modes of the signal. Such a narrow bandwidth is automatically determined and is dependent on the input signal and the cutoff frequency design. Table 3 presents the orthogonalization coefficients between the signal undergone the bandpass-EMD filter after combining all IMFs generated by EEMD with 0%, 5%, 10%, 20%, and 40% noise levels,

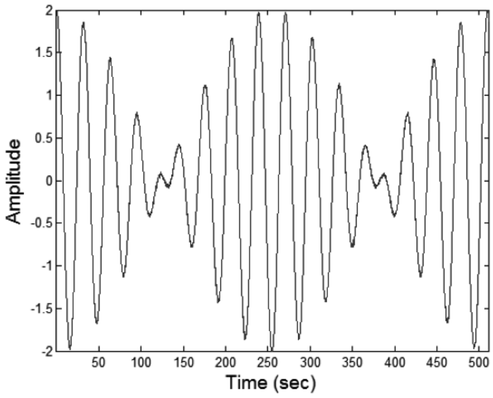

Combined all IMFs

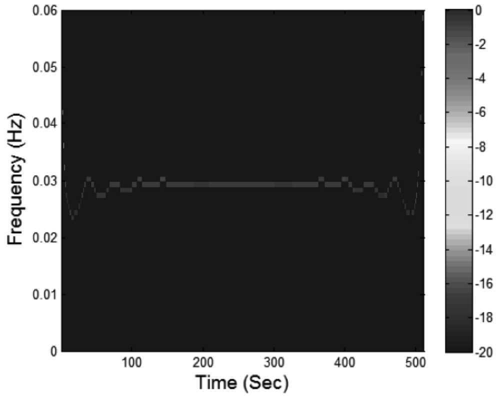

Hilbert spectrum after bandpass (mode 1)

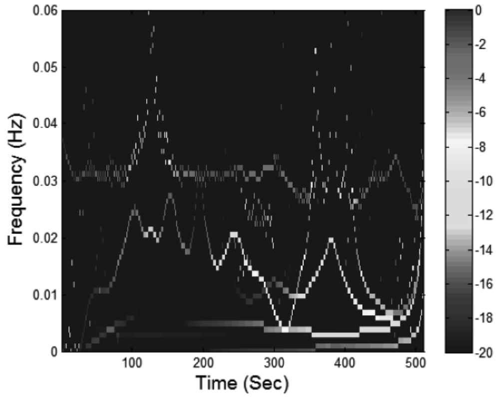

Hilbert spectrum of combined all IMFs

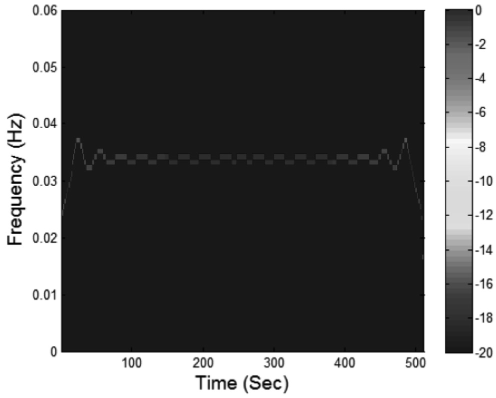

Hilbert spectrum after bandpass (mode 2)

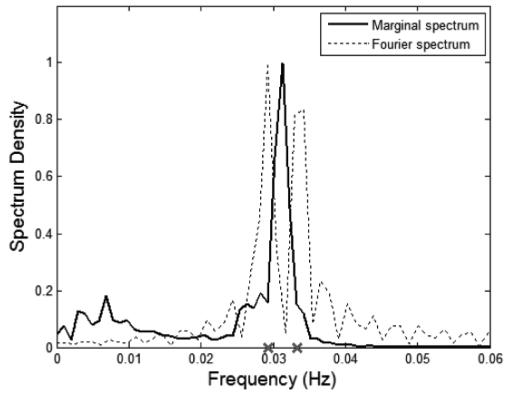

Marginal spectrum of combined all IMFs

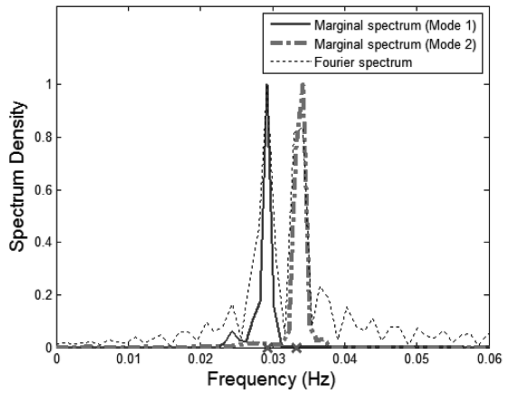

Marginal spectrum after bandpass

Fig. 4 The Hilbert spectra and marginal spectra of the signal containing combined all IMFs generated by EEMD with 20% noise level (left portion) and the correspondingly filtered signal after the bandpass-EMD filter (right portion), respectively (× indicate the real modal frequencies)

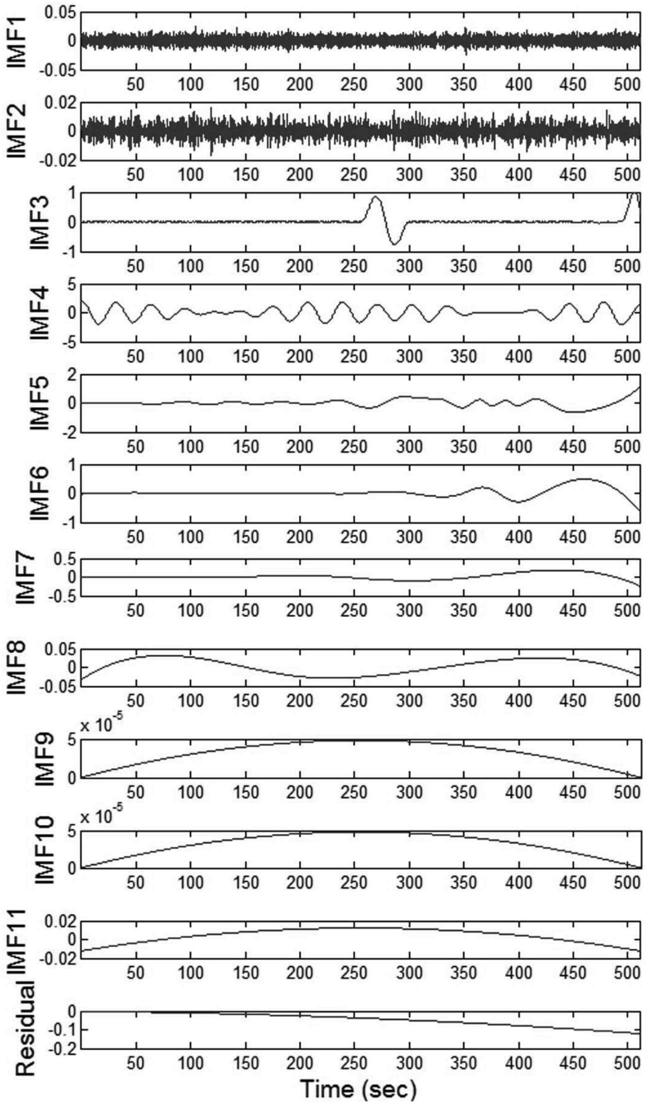

Fig. 5 The decomposed IMFs of the signal containing combined all IMFs generated by EEMD with 20% noise level

respectively, and the decomposed IMFs, for mode 1 and mode 2 evaluation. The bandpass-EMD filter has successfully solved the mode mixing problem to produce two distinguished modes, with the orthogonalization coefficients of the selected IMF1 equal to 0.4995 and 0.5000 (highest value) for mode 1 and mode 2, respectively, as listed in Table 3, thereby indicating that IMF1 best represents the modal signal.

The effectiveness of the bandpass-EMD filter can be illustrated by comparing the 3 Hilbert spectra obtained: (1) from the signal containing combined all IMFs generated by EEMD with 20% noise level to result in the Hilbert spectrum (middle left of Fig. 4), (2) and the correspondingly filtered signal after the bandpass-EMD filter to result in the two Hilbert spectra of mode 1 (upper

Table 2 Orthogonalization coefficients between the signal containing combined all IMFs generated by EEMD with 0%, 5%, 10%, 20%, and 40% noise levels, respectively, and the decomposed IMFs

	0% Noise	5% Noise	10% Noise	20% Noise	40% Noise
Self	0.5	0.5	0.5	0.5	0.5
IMF1	**0.4995**	0.0000	0.0000	0.0000	0.0003
IMF2	0.0046	0.0036	0.0000	0.0000	0.0001
IMF3	-0.0009	**0.4916**	**0.3430**	**0.0630**	0.0000
IMF4	-0.0004	0.0304	**0.1140**	**0.4885**	**0.4890**
IMF5	-0.0002	-0.0083	-0.0190	0.0186	0.0048
IMF6	0.0000	-0.0073	-0.0037	-0.0083	0.0248
IMF7	0.0000	-0.0030	-0.0010	-0.0030	-0.0021
IMF8	0.0000	0.0000	0.0000	-0.0005	-0.0017
IMF9	0.0000	-0.0013	0.0000	0.0000	0.0000
IMF10	0.0000	0.0000	0.0000	0.0000	0.0000
IMF11	0.0000	-0.0006	0.0000	-0.0001	0.0000
Residual	-0.0002	-0.0026	-0.0008	-0.0010	-0.0023

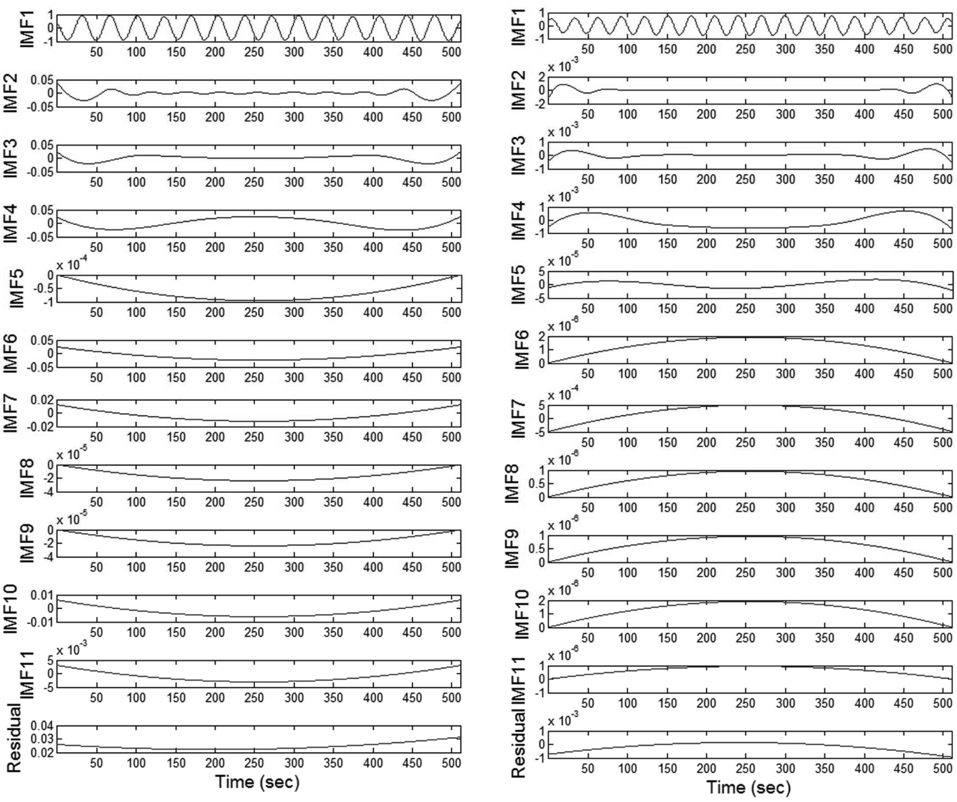

Fig. 6 The decomposed IMFs of mode 1 (left portion) and mode 2 (right portion), respectively, for the signal undergone the bandpass-EMD filter after combining all IMFs generated by EEMD with 20% noise level

Table 3 Orthogonalization coefficients between the signal undergone the bandpass-EMD filter after combining all IMFs generated by EEMD with 0%, 5%, 10%, 20%, and 40% noise levels, respectively, and the decomposed IMFs, for mode 1 and mode 2 evaluation

Mode 1	0% Noise	5% Noise	10% Noise	20% Noise	40% Noise
Self	0.5	0.5	0.5	0.5	0.5
IMF1	**0.4995**	**0.4995**	**0.4995**	**0.4995**	**0.4995**
IMF2	0.0002	0.0002	0.0002	0.0002	0.0002
IMF3	-0.0001	-0.0001	-0.0001	-0.0001	-0.0001
IMF4	-0.0003	-0.0003	-0.0003	-0.0003	-0.0003
IMF5	0.0000	0.0000	0.0000	0.0000	-0.0006
IMF6	-0.0006	0.0000	0.0000	-0.0006	-0.0003
IMF7	0.0000	-0.0006	0.0000	-0.0003	-0.0001
IMF8	0.0000	0.0000	0.0000	0.0000	-0.0001
IMF9	0.0000	0.0000	0.0000	0.0000	0.0000
IMF10	0.0000	0.0000	-0.0006	-0.0001	0.0000
IMF11	0.0000	-0.0003	0.0000	-0.0001	0.0000
Residual	-0.0012	-0.0009	-0.0012	-0.0007	-0.0007
Mode 2	0% Noise	5% Noise	10% Noise	20% Noise	40% Noise
Self	0.5	0.5	0.5	0.5	0.5
IMF1	**0.5000**	**0.5000**	**0.5000**	**0.5000**	**0.5000**
IMF2	0.0000	0.0000	0.0000	0.0000	0.0000
IMF3	0.0000	0.0000	0.0000	0.0000	0.0000
IMF4	0.0000	0.0000	0.0000	0.0000	0.0000
IMF5	0.0000	0.0000	0.0000	0.0000	0.0000
IMF6	0.0000	0.0000	0.0000	0.0000	0.0000
IMF7	0.0000	0.0000	0.0000	0.0000	0.0000
IMF8	0.0000	0.0000	0.0000	0.0000	0.0000
IMF9	0.0000	0.0000	0.0000	0.0000	0.0000
IMF10	0.0000	0.0000	0.0000	0.0000	0.0000
IMF11	0.0000	0.0000	0.0000	0.0000	0.0000
Residual	0.0000	0.0000	0.0000	0.0000	0.0000

right of Fig. 4) and mode 2 (middle right of Fig. 4). Either the outcome of the original signal using EEMD (middle right of Fig. 2) or the outcome of the signal containing combined all IMFs generated by EEMD (middle left of Fig. 4) appears to be contaminated with noise and difficult to determine the embedded two modes as shown in their corresponding marginal spectra. After the bandpass-EMD filtering, the real modes can be identified in the marginal spectrum. Fig. 6 shows the consequently decomposed IMFs (using EMD) of mode 1 (left portion) and mode 2 (right portion), respectively, for the signal undergone the bandpass filter after combining all IMFs generated by EEMD with 20% noise level. The IMF1 is selected for both modes when checking its orthogonalization coefficient as listed in Table 3 and shown in Fig. 6. Such a selected IMF

Table 4 Estimated frequencies of the two-mode signal using FFT for the original signal, EEMD for the original signal, EMD for combined all IMFs generated by EEMD, and bandpass-EMD for combined all IMFs generated by EEMD, respectively

Noise		Frequency (Hz)		Relative Error		Average Relative Error
		Mode 1	Mode 2	Mode 1	Mode 2	
	Real	0.02941	0.03333			
0%	FFT	0.02930	0.03419	0.37%	2.56%	1.47%
	EEMD	0.03125	0.03125	6.25%	6.25%	6.25%
	EMD	0.03125	0.03125	6.25%	6.25%	6.25%
	Bandpass-EMD	0.02930	0.03418	0.39%	2.54%	**1.46%**
5%	FFT	0.02930	0.03419	0.37%	2.56%	1.47%
	EEMD	0.03027	0.03027	2.93%	9.18%	6.05%
	EMD	0.03125	0.03125	6.25%	6.25%	6.25%
	Bandpass-EMD	0.02930	0.03418	0.39%	2.54%	**1.46%**
10%	FFT	0.02930	0.03419	0.37%	2.56%	1.47%
	EEMD	0.03125	0.03125	6.25%	6.25%	6.25%
	EMD	0.03027	0.03027	2.93%	9.18%	6.05%
	Bandpass-EMD	0.02930	0.03418	0.39%	2.54%	**1.46%**
20%	FFT	0.02930	0.03419	0.37%	2.56%	1.47%
	EEMD	0.03027	0.03027	2.93%	9.18%	6.05%
	EMD	0.03125	0.03125	6.25%	6.25%	6.25%
	Bandpass-EMD	0.02930	0.03418	0.39%	2.54%	**1.46%**
40%	FFT	0.02930	0.03419	0.37%	2.56%	1.47%
	EEMD	0.03125	0.03125	6.25%	6.25%	6.25%
	EMD	0.00195	0.00195	93.36%	94.14%	93.75%
	Bandpass-EMD	0.02930	0.03418	0.39%	2.54%	**1.46%**

represents a simple oscillatory mode embedded in the signal (Huang *et al*. 1999, Lei and Zuo 2009).

Table 4 lists the final estimated frequencies of the two-mode signal using FFT for the original signal, EEMD for the original signal, EMD for the signal containing combined all IMFs generated by EEMD, and bandpass-EMD for the signal containing combined all IMFs generated by EEMD, respectively. Obviously, the bandpass-EMD has solved the mode mixing problem. In fact, directly applying EEMD or EMD will produce one "averaged" modal frequency with a higher average relative error of either 6.05% or 6.25%, when compared to that of 1.46% and 1.47% using the bandpass-EMD and FFT, respectively. Regardless of the signal with 0%, 5%, 10%, 20%, or 40% noise level, the bandpass-EMD algorithm is able to achieve accurate and stable results in modal frequency estimation, which is characteristic of a robust filter.

3.2 Evaluation of a real bridge structure

The proposed approach is also applied to a real bridge structure (e.g., Mao-Luo-Hsi Bridge in

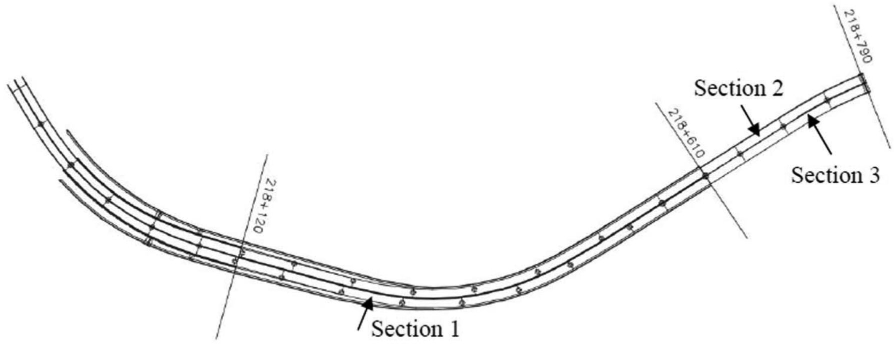

Fig. 7 Location of ambient vibration test on Mao-Luo-Hsi Bridge

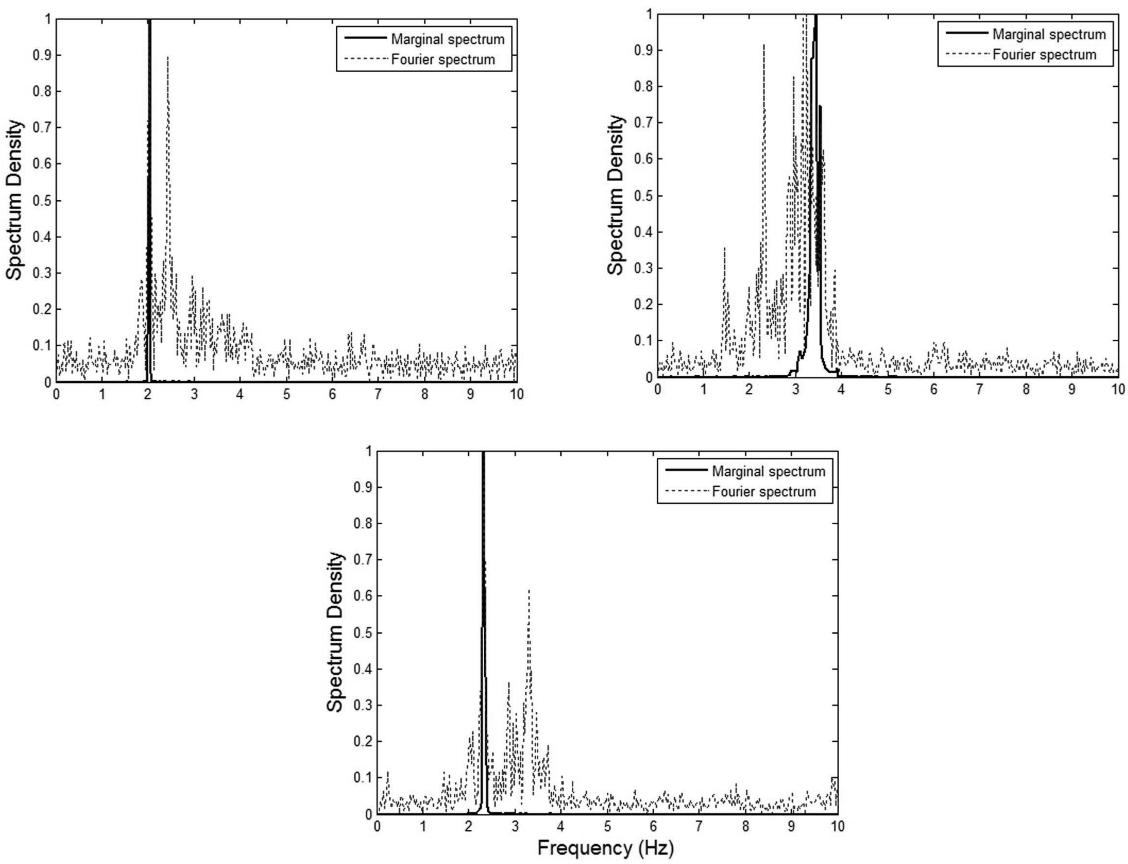

Fig. 8 Marginal spectrum vs. Fourier spectrum of Mao-Luo-Hsi Bridge (from top to bottom refers to the indicated section 1, section 2, and section 3 of the bridge, respectively)

Nantou county of Taiwan) to evaluate the principal frequency of the bridge in the longitudinal direction. Three sections of the bridge deck (Fig. 7) are chosen and subjected to ambient vibrations, with the sampling time interval Δt = 0.005 s. As the ambient vibration test is easily influenced by

Table 5 Estimated principal frequencies of Mao-Luo-Hsi Bridge in sections 1-3 using FFT, EMD, and bandpass-EMD, respectively

	Section 1	Section 2	Section 3
FFT	2.0269	3.2479	2.3443
EMD	7.9038	1.0934	5.9981
Bandpass-EMD	2.0306	3.4364	2.3118

the surrounding environment resulting from a slight vibration force, the measured signals are susceptible to interference, such as vehicles passing through during measurement, and thus contaminated by noise. Hence, it is beneficial to directly adopt the bandpass-EMD approach to preprocess the contaminated signals by the bandpass filter, followed by the mode extraction using EMD and evaluation of the mode in the marginal spectrum. It is noted that the EEMD process is omitted in this case since the optimal noise level producing the best outcomes of EEMD is usually not available and requires a considerable amount of time to properly train the algorithm.

Fig. 8 shows the marginal spectrum vs. Fourier spectrum of Mao-Luo-Hsi Bridge (from top to bottom refers to the indicated section 1, section 2, and section 3 of the bridge, respectively). It is clear to see that there are a few local peaks in amplitude representing possible modes in each frequency spectrum. However, these local peaks can be attributed to vehicles passing through during measurement, and thus only the global peak is selected to represent its principal frequency. Table 5 lists the estimated principal frequencies of Mao-Luo-Hsi Bridge in sections 1-3 using the FFT, EMD, and bandpass-EMD, respectively. The results of the bandpass-EMD are quite close to those of FFT while the outcomes of the pure EMD demonstrate some deviations, implying that the bandpass-EMD approach is able to acquire more reliable results than the pure EMD.

4. Discussions on the determination of mode number

The bandpass filter for the signal in Eq. (10) is designed to allow two zones of oscillations (pass-bands), as the signal contains two remarkable peaks in the frequency spectrum. The Fourier spectrum of the original signal in Fig. 2 tells that there are two peaks, indicating two modes for the two-mode signal that represents a stationary system. Hence, the Fourier spectrum components can assist in determining the mode number for a stationary process. For non-stationary systems, the local spectrum components are not corresponding to the true frequencies. In such cases, a criterion to determine the possible number of modes for the signal of interest is developed that springs from the works by Peng *et al*. (2005) and Bao *et al*. (2009), who presented a selection criterion for IMFs decomposed from the signal based on the correlation coefficient, μ_n $(n = 1, 2, \ldots, N;$ N is the number of IMFs), between each IMF and the signal to be processed. A threshold ρ is defined as

$$\rho = \frac{\max(\mu_n)}{\eta}, \quad n = 1, 2, \ldots, N \tag{11}$$

where η is a factor lager than 1.0 and is usually decided empirically. The criterion is to keep the nth IMF as the mode if $\mu_n \geq \rho$, while eliminate the remaining IMFs. By using the η equal to 10 (Peng *et al*. 2005) and substituting the correlation coefficient with the orthogonalization coefficient used in this study, Eq. (11) becomes

$$\rho = \frac{\max(\mathrm{IO}_n)}{10}, \quad n = 1, 2, \ldots, N \tag{12}$$

The IMFs decomposed using EEMD tells that there are two "distinguished" modes available for the cases of the signal adding 5%, 10%, 20%, and 40% noise levels as listed in Table 1 (in bold). However, such results for determining the mode number cannot be confirmed in each of their corresponding marginal spectra, only showing one "averaged" mode, as shown in Fig. 2 for the case of 20% noise level for instance. This condition cannot be improved until the bandpass-EMD filter is adopted to extract the true modes of the signal.

5. Conclusions

A hybrid algorithm based on EEMD and bandpass-EMD has been developed to interpret the possibility of multi-mode distribution of the IMFs decomposed using EEMD. A simulated signal with two-modes is tested to demonstrate the efficiency of the hybrid algorithm. The noise level with a standard deviation of 0%, 5%, 10%, 20%, and 40% relative to the original signal is first added to the signal, respectively. The signal is then decomposed into IMFs using the EEMD, followed by combining the multi-mode into a single mode, and sifting it again to produce proper IMFs, each representing a mode using the bandpass-EMD filter that divides the outcome of EEMD into different groups for mode evaluation. The estimated frequencies of the two-mode signal are compared with the real values. Comparisons of the estimated frequencies are made between the algorithms using (1) FFT for the original signal, (2) EEMD for the original signal, (3) EMD for the signal containing combined all IMFs generated by EEMD, and (4) bandpass-EMD for the signal containing combined all IMFs generated by EEMD, respectively. It has proven that the bandpass-EMD filter is capable of solving the mode mixing problem: directly applying EEMD or EMD will produce one "averaged" modal frequency with a higher average relative error of either 6.05% or 6.25%, when compared to that of 1.46% and 1.47% using the bandpass-EMD and FFT, respectively. Regardless of the noise level added to the signal, the bandpass-EMD algorithm is able to achieve accurate and stable results in modal frequency estimation, which is characteristic of a robust filter. The bandpass-EMD filter has also demonstrated the grouping efficiency for the combined IMFs generated by EEMD and for the signal when the EMD is directly adopted, and thereby the efficiency of mode determination for multi-mode signals. On the other hand, the EEMD algorithm cannot reach satisfactory results until the "best" one is selected after several trials of noise levels have been conducted. Discussions on the determination of modes, for both stationary and non-stationary systems, are offered to explain the connection between mode-grouping form and type on the one hand, and mode-grouping performance on the other. Furthermore, a real bridge structure subjected to ambient vibrations whose responses are easily contaminated with noise is tested to verify the efficiency of the bandpass-EMD algorithm, showing its ability to acquire more reliable results than the pure EMD.

Acknowledgements

This research study was sponsored by the National Science Council, Taiwan, R.O.C. (research grant NSC 97-2221-E-035-045) whose support was greatly appreciated. Special thanks are due to the EMD/EEMD evaluation code by Wu and to the Hilbert spectrum evaluation code by Gabriel.Rilling (at) ens-lyon.fr. The author is also most grateful for the kind assistance of Prof. Chang-Koon Choi, Editor of SEM, and the constructive suggestions of the anonymous reviewers all of which has led to the making of several corrections and suggestions that have greatly aided me in the presentation of this paper.

References

Bao, C., Hao, H., Li, Z.X. and Zhu, X. (2009), "Time-varying system identification using a newly improved HHT algorithm", *Comput. Struct.*, **87**(23-24), 1611-1623.

Chen, L., Li, X., Li, X.B. and Huang, Z.Y. (2009), "Signal extraction using ensemble empirical mode decomposition and sparsity in pipeline magnetic flux leakage nondestructive evaluation", *Rev. Sci. Instrum.,* **80**(2), 025105.

Etter, D.M. (1993), *Engineering Problem Solving with MATLAB*, Prentice-Hall.

Flandrin, P., Rilling, G. and Gonçalvès, P. (2004), "Empirical mode decomposition as a filter bank", *IEEE Signal Proc. Let.,* **11**, 112-114.

Gledhill, R.J. (2003), "Methods for investigating conformational change in biomolecular simulations", Ph.D. Thesis, the University of Southampton, UK.

Huang, N.E., Shen, Z., Long, S.R., Wu, M.C., Shih, H.H., Zheng, Q., Yen, N.C., Tung, C.C. and Liu, H.H. (1998), "The empirical mode decomposition and the Hilbert spectrum for nonlinear and non-stationary time series analysis", *Proc. R. Soc. London,* **454**, 903-995.

Huang, N.E., Shen, Z. and Long, S.R. (1999), "A new view of nonlinear water waves: the Hilbert spectrum", *Annu. Rev. Fluid Mech.,* **31**, 417-457.

Huang, N.E., Wu, M.C., Long, S.R., Shen, S.P., Qu, W., Gloersen, P. and Fan, K.L. (2003), "A confidence limit for the empirical mode decomposition and Hilbert spectral analysis", *Proc. R. Soc. London,* **459**, 2317-2345.

Lei, Y. and Zuo, M.J. (2009), "Fault diagnosis of rotating machinery using an improved HHT based on EEMD and sensitive IMFs", *Meas. Sci. Technol.,* **20**(12), 1-12.

Li, Y.Y., Niu, D.X., Qi, J.X. and Liu, D. (2008), "A novel hybrid power load forecasting method based on ensemble empirical mode decomposition", *Power Syst. Technol.*, **32**(8).

Lin, J.W. (2010), "Mode-by-mode evaluation of structural systems using a bandpass-HHT filtering approach", *Struct. Eng. Mech.*, **36**(6), 697-714.

Peng, Z.K., Tse, P.W. and Chu, F.L. (2005), "A comparison study of improved Hilbert-Huang transform and wavelet transform: Application to fault diagnosis for rolling bearing", *Mech. Syst. Signal Pr.*, **19**, 974-988.

Wu, Z. and Huang N.E. (2004), "A study of the characteristics of white noise using the empirical mode decomposition method", *Proc. R. Soc. London*, **460A**, 1597-1611.

Wu, T.Y. and Chung, Y.L. (2009), "Misalignment diagnosis of rotating machinery through vibration analysis via the hybrid EEMD and EMD approach", *Smart Mater. Struct.*, **18**(9), 095004.

Wu, Z. HHT MATLAB Program. Website: http://rcada.ncu.edu.tw/research1_clip_program.htm.

Wu, Z. and Huang, N.E. (2009), "Ensemble empirical mode decomposition: a noise assisted data analysis method", *Adv. Adapt. Data An.*, **1**(1), 1-41.

Xu, Y.L., Chen, S.W. and Zhang, R.C. (2003), "Modal identification of Di Wang Building under typhoon york using the Hilbert-Huang transform method", *Struct. Des. Tall Spec. Build.,* **12**, 21-47.

Yeh, J.R., Lin, T.Y., Shieh, J.S., Chen, Y., Huang, N.E., Wu, Z. and Peng, C.K. (2008), "Investigating complex patterns of blocked intestinal artery blood pressure signals by empirical mode decomposition and linguistic analysis", *J. Phys. Conf. Series,* **96**, 012153.

Zhang, X., Lai, K.K. and Wang, S.Y. (2008), "A new approach for crude oil price analysis based on empirical mode decomposition", *Energy Economics*, **30**(3), 905-918.

Zhou, X., Zhao, H. and Jiang, T. (2009), "Adaptive analysis of optical fringe patterns using ensemble empirical mode decomposition algorithm", *Optics Letters*, **34**(13), 2033-2035.